

# PROPERTY AND THERMOSTABILITY STUDY ON TC6 TITANIUM ALLOY NANOSTRUCTURE PROCESSED BY LSP

Wang Xuede, Li Yinghong, Li Qipeng, He Weifeng, Nie Xiangfan, Li Yuqin

(Science and Technology on Plasma Dynamics Laboratory, Air Force Engineering University, Xi'an, 710038, P. R. China)

**Abstract:** TC6 titanium alloy samples are processed by laser shock peening (LSP). Then, some samples are vacuum annealed at 623 K for 10 h for the study on the thermostability of the nanostructure produced by LSP. The characteristics of the strengthened layer and nanostructure are studied by atomic force microscopy (AFM), scanning electron microscope (SEM), electron backscatter diffraction (EBSD), X-ray diffraction (XRD), and transmission electron microscopy (TEM) appliances, meanwhile the enhanced microhardness is tested at cross section. AFM of the processed surface indicates that the deformation is approximately uniform, and LSP slightly increases the roughness. SEM and EBSD of the strengthened cross section show that  $\alpha$  phases are compressed to strip-shaped, a proportion of  $\alpha$  and  $\beta$  phases is shattered to smaller phases from surface to 200  $\mu\text{m}$  in depth. The surface XRD shows that although there is no new produced phase during LSP, the grain size refinement and the introduction of lattice micro-strains lead to the broadened peak. The TEM photographs and diffraction patterns indicate that the shock wave provides high strain rate deformation and leads to the formation of nanocrystal. Compared with the samples before annealing, the dislocation density is lower and the grain-boundary is more distinct in the annealed samples, but the nanocrystal size does not grow bigger after annealing. The microhardness measurement indicates that LSP improves the microhardness of TC6 for about 12.2% on the surface, and the layer affected by LSP is about 500  $\mu\text{m}$  in depth. The microhardness after annealing is 10  $\text{HV}_{0.5}$  lower, but the affected depth does not change. The thermostable study shows that the strengthened layer of TC6 processed by LSP is stable at 623 K. The strengthened thermostable layer can significantly improve the fatigue resistance, wear resistance and stress corrosion resistance of the titanium alloy. The study results break the USA standard AMS2546 that titanium parts after LSP are subjected in subsequent processing within 589 K.

**Key words:** laser shock peening (LSP); TC6 titanium alloy; nanostructure; microhardness; thermostability

**CLC number:** V216.3

**Document code:** A

**Article ID:** 1005-1120(2012)01-0068-09

## INTRODUCTION

In contrast to steel, the mechanical performance of titanium alloys is very attractive with combinations of strength, toughness, fatigue, and outstanding corrupting resistance. Titanium alloys have been widely used in aero industry, especially in aero-engines, which have already replaced the aluminum alloys and stainless steel to a certain extent<sup>[1]</sup>. However, titanium alloys are very sensitive to minor defects and stress concentration, which results in the failure of the aero-engine components<sup>[2-6]</sup>.

Many surface treatment technologies such as laser-quenching, ion implantation and shot peening have been used to improve the fatigue abilities of titanium alloys<sup>[7-12]</sup>. Among the above traditional surface treatment technologies, shot peening is the most effective and widely used. Shot peening is relatively inexpensive, uses robust process equipment, and can be used on large or small areas as required. However, the shot peening process has its limitations. In determining the produced compressive stresses, the process is semi-quantitative and depends upon a metal strip or gage called an Almen type gage to provide an indi-

cation of shot peening intensity. Firstly, this gage does not guarantee that the shot peening intensity is uniform across the peened component. Secondly, the compressive residual stresses are limited in depth, usually not exceeding 0.25 mm in soft metals such as aluminum alloys and less in titanium alloys. Thirdly, the peening process results in a roughened surface, even sometimes minor cracks. This roughness needs to be removed before use in wear applications. The used typical processes remove the majority of the compressive layer<sup>[13]</sup>. An alternative novel surface processing technology, namely laser shock peening (LSP), can induce greater depth of residual stress and produce strengthening nanostructure into metal surfaces using high-power, Q-switched laser pulses.

LSP used to shock TC4 titanium alloy has been vastly studied by researchers in domestic and abroad<sup>[14-19]</sup>. LSP induced compressive residual stress distribution in TC4 as well as its mechanism to prolong the target fatigue life was studied in detail<sup>[15,18]</sup>. However, as one of the most important titanium alloys used in China, LSP of TC6 has not been studied yet. In this paper, the pattern of nanostructure, the characteristic of the enhanced microhardness and the thermostability of TC6 titanium alloy processed by LSP are studied in detail.

## 1 EXPERIMENTAL DETAILS

### 1.1 Principle and experimental procedure of LSP

During LSP, the laser beam is directed onto the treated surface, it passes through the transparent confining medium (water/glass) and strikes the sample. A short laser pulse is then focused onto the sample to immediately vaporize the ablation medium. The energy absorption at the confining medium/plasma interface leads to the formation of a shock wave which strikes the sample with an intensity of several Gigapascals. The high pressure against the surface of the sample causes a shock wave to propagate into the material. The plastic deformation caused by the shock

wave produces the compressive residual stress, nano-crystallization and hardness enhancement on the surface of the sample<sup>[17-19]</sup>. LSP has been proved effective in improving material fatigue strength in a number of alloys<sup>[20-24]</sup>. The use of LSP has been proposed, and in some implemented cases, as a localized surface treatment for airfoils in the fan sections of certain military aircraft engines that are particularly sensitive to foreign object damage (FOD) induced high cycle fatigue (HCF) failures<sup>[25]</sup>.

### 1.2 Preparation of test samples

TC6 is primarily composed of the hexagonal close-packed (HCP)  $\alpha$  phases and the body-centered cubic  $\beta$  phases. Both two kinds of phases are of equiaxed grains. Fig. 1 is the metallographic of the titanium without LSP, the white regions are  $\alpha$  phases and the black regions are  $\beta$  phases. The composition of TC6 titanium alloy is shown in Table 1<sup>[26]</sup>.

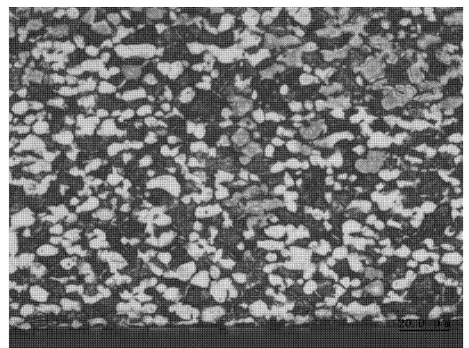


Fig. 1 Metallographic of original TC6 without LSP

**Table 1** Composition of TC6 titanium alloy wt%

Composition	Al	Mo	Cr	Fe	Si	Ti
Percent	5.5-7.0	2.0-3.0	0.8-2.3	0.2-0.7	0.15-0.40	Bal

The test sample is mounted on a five-coordinate table controlled in  $x$ - $y$  direction with floating water as confining medium. During LSP, the shock waves are induced by a Q-switched laser system based on a neodymium-doped glass and yttrium aluminum garnet (YAG) crystal lasing rod which operates in the near infrared with a wavelength of 1 054 nm and a pulse of around 20 ns. The LSP parameters to process the sample are listed in Table 2.

**Table 2** LSP parameters

Parameter	Value
Laser wavelength/nm	1 064
Pulse energy/J	6
Pulse duration/ns	20
Spot diameter/mm	3
Repetition-rate/Hz	1
System ASE energy/mJ	<50
Export laser energy stability/%	< $\pm 5$
Lapping rate/%	70

According to the previous experiments, the sample surface is laser processed with spots of 3 mm in diameter moving forward along the work piece. Samples are treated with three layers at the same power density ( $4.24 \text{ GW/cm}^2$ ). The standard after LSP is that; Macro-deformation should not happen, dimension of samples should not change, and roughness with LSP should satisfy project application. Then, some of samples treated by LSP are vacuum annealed at 623 K for 10 h.

### 1.3 Measurement equipments and methods

The characteristics of TC6 layer before and after LSP are measured by Dimension-3100 atomic force microscope (AFM) and electron backscatter diffraction (EBSD). And the nanostructures induced by LSP with and without annealing are studied using JEOL/JSM-6360LV scanning electron microscope (SEM) and TEM-3010 transmission electron microscope (TEM). XRD-7000 X-ray diffraction (XRD) equipment is used to study the diffraction patterns. The Vickers microhardness (HV) measurements are made on a MVS-1000JMT2 microhardness tester using an indentation load of 500 g at cross section, a dwell time of 10 s.

## 2 RESULTS AND DISCUSSION

### 2.1 AFM observation

The typical deformed configuration of the shocked region is observed and measured using AFM, as seen in Fig. 2. The deformation is approximately uniform along the shocked line, which is indicative of a 3-D deformation state.

From both 3-D geometry and height information in Fig. 2, the altitude variation is only  $0.06 \mu\text{m}$ . It is clear that LSP slightly increases the roughness, and there are no defects such as ablation and minor cracks produced by LSP. Since the surface integrality and the low roughness are significant to the wear and the fatigue performances of TC6 titanium alloy, the selected LSP parameters are beneficial to the titanium alloy.

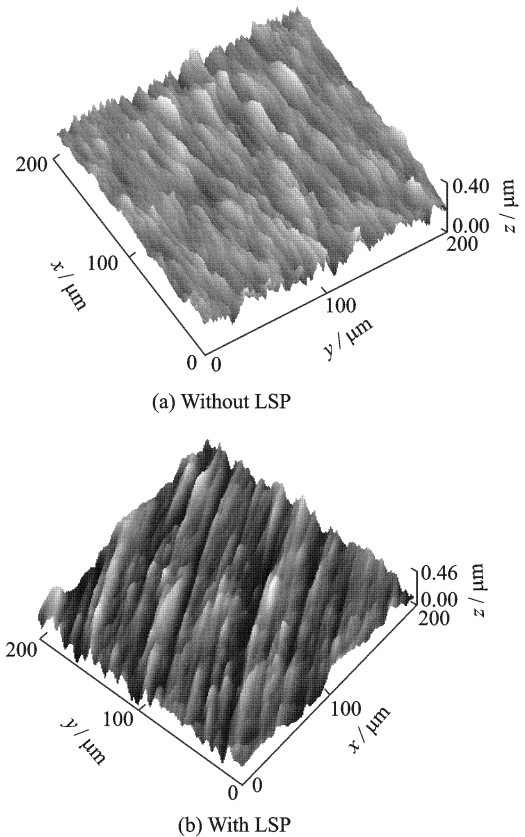
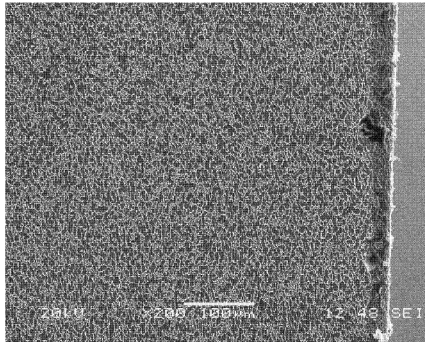


Fig. 2 3-D shapes without and with LSP

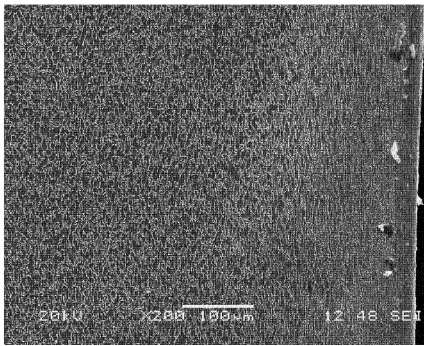
### 2.2 SEM and EBSD observation

Fig. 3(a) is the SEM morphology of the sample cross section without LSP. Over 50% equiaxed  $\alpha$  phases evenly distribute in the material and a quantity of  $\beta$  phases unevenly distribute among  $\alpha$  phases. Fig. 3(b) is the SEM morphology of the sample cross section with three LSP layers at power density of  $4.24 \text{ GW/cm}^2$ . In this picture, the severe plastic deformation (SPD) layer and substrate can be distinguished easily. The SPD layer is about  $200 \mu\text{m}$ . The  $\alpha$  phases are elongated by normal shock wave to the surface and the  $\beta$  phases are shattered in the SPD layer.

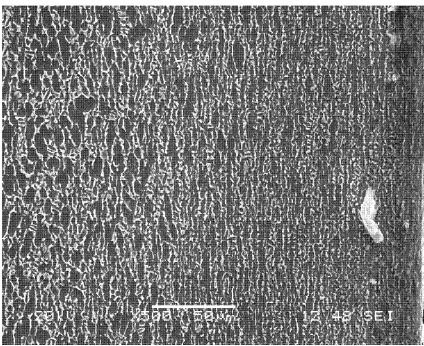
Fig. 3(c) is the SEM morphology of the sample cross section after annealing. Paired observing Figs. 3(b,c), it can be seen that the depth of SPD layer does not decrease after annealing. Fig. 3(d) is the partial enlarged detail of Fig. 3(c), the patterns of  $\alpha$  and  $\beta$  phases do not change either.



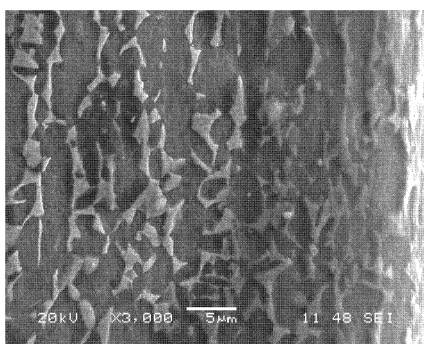
(a) Without LSP



(b) Three LSP layers



(c) LSP+annealing

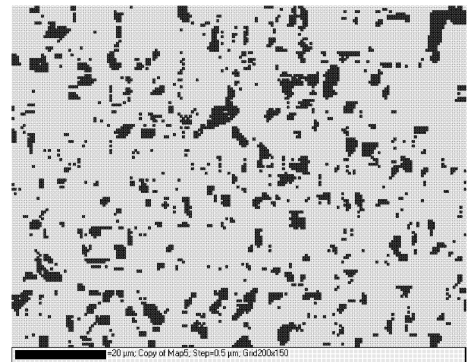


(d) Partial enlarged detail of (c)

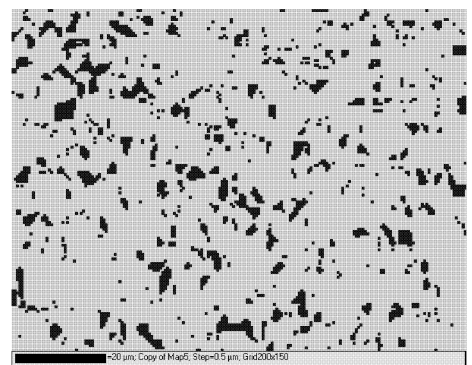
Fig. 3 SEM morphologies of cross section

EBSD is a diffraction technique for obtaining crystallographic orientation with sub-micron spatial resolution from bulk samples or thin layers in SEM<sup>[27]</sup>.

The crystallographic orientation of the surface microstructure is collected using EBSD, which provides information about the lattice rotation during LSP, as shown in Fig. 4. The white regions correspond to the  $\alpha$  phases and the black regions correspond to the  $\beta$  phases respectively. As can be seen in Fig. 4(b), lattice rotation due to the high plasma shock wave leads to a dominance orientation distribution of the two kinds of phases, but there is no new produced phase.



(a) Without LSP

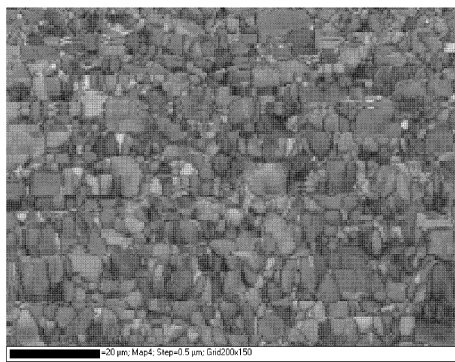


(b) Three LSP layers

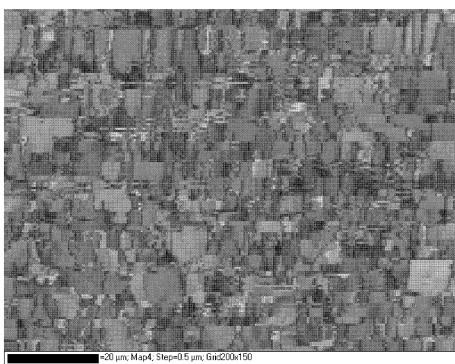
Fig. 4 EBSD of TC6 surface without and with LSP

The EBSD diffraction patterns at cross section without and with LSP are shown in Fig. 5. Compared with Fig. 5(a), the low diffraction quality of Fig. 5(b) reveals that SPD happens at the surface layer during LSP, and the affected layer is about 200  $\mu\text{m}$ . As we can see in Fig. 5(b), the  $\alpha$  phases are compressed and stretched in the strengthened layer, and a proportion of  $\alpha$  and  $\beta$  phases is shattered to smaller phas-

es. The compressed phases induce compressive residual stress at the surface layer. The residual compressive stress with the strengthening phases together restrains initiation and propagation of the fatigue cracks during low cycle fatigue (LCF) and high cycle fatigue (HCF), thus improving the fatigue performance and increasing the fatigue life of the titanium alloy.



(a) Without LSP



(b) Three LSP layers

Fig. 5 EBSD diffraction patterns at cross section

## 2.3 XRD observation

Since the shallow nanostructure produced by LSP and the bigger  $\theta$  angle in routine XRD lead to the shortened distance of X-ray in the strengthened layer, a new film-XRD method is used to measure the diffraction patterns. Fig. 6 is the XRD patterns with different layers. It can be seen that there is no additional peak with different LSP layers, which indicates that no phase transformation and no new crystalline phases are formed when high pressure laser shock wave transmits in the material. The main phases are  $\alpha$  and  $\beta$ . The second interesting feature in XRD patterns is that the peaks are broadened with LSP. The peak broadening indicates the grain size refinement and

the introduction of lattice microstrains<sup>[28]</sup>. The main reason is that the high strain rate can generate high density dislocation and cold work in the material. This consists with the phenomenon in nanocrystalline materials prepared via the other SPD methods. In the SPD zone, there are high internal stresses<sup>[29]</sup>. As a result, XRD line broadening of these nc-materials is due to crystallite refinement, lattice microstrains and instrumental broadening.

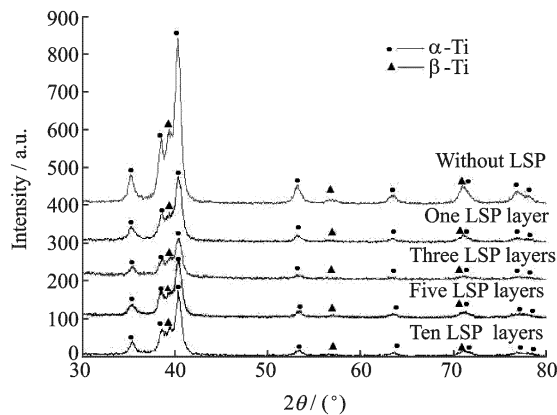
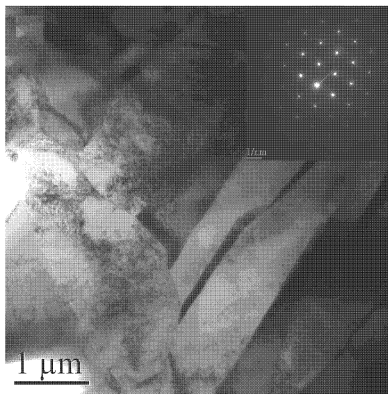


Fig. 6 XRD patterns of TC6 with different LSP layers

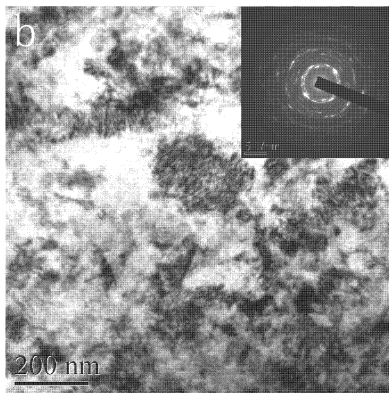
## 2.4 TEM observation

The nanostructure changes of the current titanium alloy induced by LSP and annealing are shown in Fig. 7.

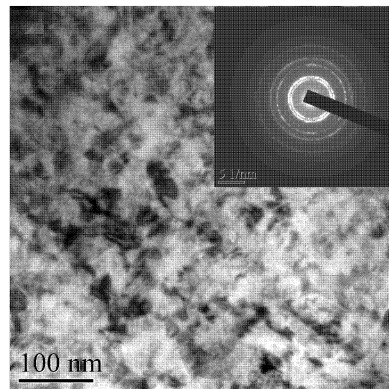
Fig. 7(a) presents the original features of the sample without LSP. The diffusive diffraction spots in the SAED pattern are identified as  $\alpha$  phases. Fig. 7(b) is the diffraction pattern and TEM micrograph near the surface processed by LSP, and TEM micrograph shows a very high density dislocation region and dislocation cells. The diffraction patterns reveal that dislocation cells are large and have thin walls composed of tangled dislocations in the area. Fig. 7(c) reveals that three LSP layers are enough to generate nano-grain on the surface of the titanium samples. Surface nanocrystal induced by multiple LSP is similar to those caused by SPD methods. The underlying mechanism may include: deformation localized in shear bands consisting of an array of high density dislocations, dislocation, annihilation and recombination of small-angle grain



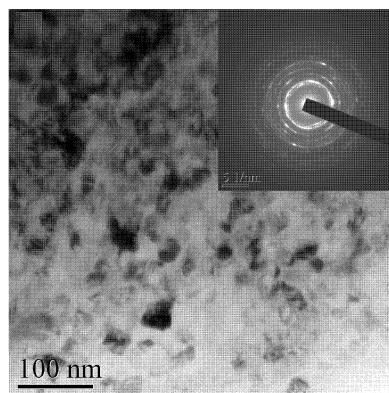
(a) Without LSP



(b) Dislocation cells produced by LSP



(c) Nano-grains produced by LSP



(d) LSP+annealing

Fig. 7 TEM photographs and diffraction patterns

to their neighboring grains becoming completely random.

Fig. 7(d) shows the features of the LSP sample vacuum annealing at 623 K for 10 h. Figs. 7(b-d) reveal that the dislocation density increases with increasing strain rate, but decreases after annealing. Furthermore, it can be seen that the nanocrystal sizes are nearly the same to those before annealing and the obscure grain-boundary becomes distinct. Therefore, it is concluded that for the nanocrystal produced by LSP, the offered energy during annealing at 623 K is not high enough to lead nano-grain boundary migration. The nanocrystal presents a barrier for dislocation movements, thus causing the dislocations to pile up and counteract at the nanocrystal boundary. It seems reasonable to assume that the amount of precipitated nanocrystals has direct effect on the mechanical property of the current titanium alloy. Therefore, the nanocrystal produced by LSP of this titanium alloy is thermostable at 623 K.

## 2.5 Microhardness test

The recorded mechanical property measurements indicate a significant increase in hardness and strength at surface layers with LSP. The hardness distribution is determined using microhardness at the cross section. Fig. 8 shows the variation in microhardness as the depth from the treated surface increases. The original hardness of TC6 titanium alloy is about 334 HV<sub>0.5</sub>. At the LSP layer of top surface, the microhardness is 406 HV<sub>0.5</sub>, which is 72 HV<sub>0.5</sub> higher than that of the matrix. The hardened depth affected by LSP is about 500 μm. After annealing the surface microhardness decreases only 10 HV<sub>0.5</sub>, and the hardened depth remains stationary. Therefore, the microhardness distribution affected by LSP of the current titanium alloy is thermostable at 623 K.

The mechanism of the hardness enhancement induced by LSP includes two factors. One is the actual increase in hardness, while the other is the introduction of residual compressive stress into

boundaries separating individual grains, and a change in the direction of the grains with respect

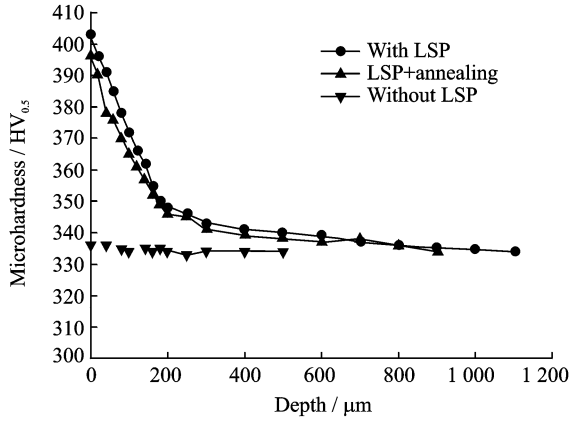


Fig. 8 Microhardness of different samples at cross section

the material during the nanocrystallization on the surface of the material. The residual stress partly releases during annealing, which leads to the minute decrease of microhardness.

### 3 CONCLUSIONS

In this paper, TC6 titanium alloy is laser shock processed and vacuum annealed at 623 K for 10 h. And the nanostructures and microhardness before and after annealing are examined. The conclusions are as follows:

(1) The processed surface AFM indicates that the selected LSP parameters are beneficial to the TC6 titanium alloy. The uniform deformation and lower roughness show that LSP is better than other traditional surface treatments.

(2) SEM and EBSD of the strengthened cross section layer show that  $\alpha$  phases are compressed and stretched at the strengthened layer, and a proportion of  $\alpha$  and  $\beta$  phases is shattered to smaller phases. The strengthened layer is about 200  $\mu\text{m}$  in depth.

(3) The surface XRD indicates that there is no new produced phase during LSP, while the grain size refinement and the introduction of lattice micro-strains with LSP lead to the broadened peak.

(4) The TEM photographs and diffraction pattern indicate that the shock wave provides high strain rate deformation and leads to the formation

of nanocrystal. Compared with the samples without annealing, the dislocation density is lower and the grain-boundary is more distinct in the annealed samples, but the size of the nanocrystal does not visibly grow larger after annealing.

(5) The microhardness measurement indicates that LSP improves the microhardness of TC6 for about 12.2% on the surface, and the hardness affected depth is about 500  $\mu\text{m}$ . The microhardness after annealing is 10 HV<sub>0.5</sub> lower, but the affected depth does not change.

(6) Tests after annealing indicate that hardness improvement and nanostructure produced by LSP are thermostable at 623 K, which is beneficial to improve the wear resistance and stay the generation of the fatigue cracks. The research production of this paper breaks the USA standard AMS2546 that titanium parts with LSP are subjected in subsequent processing within 589 K.

### References:

- [1] Ren Xudong, Zhang Yongkang, Zhou Jianzhong, et al. Study of the effect of laser shock processing on titanium alloy[J]. Huazhong Univ of Sci & Tech, 2007,35(Z1):150-152. (in Chinese)
- [2] Li Qipeng, Li Yinghong, He Weifeng, et al. Thermostability study on microstructure and microhardness of laser shock processed Ti-6Al-2.5Mo-1.5Cr-0.5Fe-0.3Si[J]. Materials Science Forum, 2012, 697/698:440-444.
- [3] Lee D, Kim S. Effects of microstructural morphology on quasi-static and dynamic deformation behavior of Ti-6Al-4V alloy[J]. Metallurgical and materials Trans A, 2001,32A(2):315-318.
- [4] Ocan'a J L, Molpeceres C, Porro J A, et al. Experimental assessment of the influence of irradiation parameters on surface deformation and residual stresses in laser shock processed metallic alloys[J]. Appl Surf Sci, 2004,238(1/4):501-505.
- [5] McCay M H, Hopkins J A. Laser surface processing of compressor blades for erosive environments[R]. AIAA 2002-1300, 2002.
- [6] Martinez S A, Sathish S, Blodgett M P, et al. X-ray diffraction residual stress measurements on surface treated Ti-6Al-4V for aerospace applications [R]. AIAA 2002-3733, 2002.

- [7] Golden P J, Hutson A, Sundaram V, et al. Effect of surface treatments on fretting fatigue of Ti-6Al-4V [J]. *Int J Fatigue*, 2007,29(7):1302-1309.
- [8] Vadiraj A, Karnaraj M. Effect of surface treatments on fretting fatigue damage of biomedical titanium alloys[J]. *Tribology Int*, 2007,40(1):82-91.
- [9] Kubiak K, Fouvry S, Wendler B G. Comparison of shot peening and nitriding surface treatments under complex fretting loadings [J]. *Mater Sci Forum*, 2006,513:105-116.
- [10] Mohrbacher H, Blanpain B, Celis J P. Friction and wear mechanisms on CVD diamond and PVD TiN coatings under fretting conditions[J]. *ASTM Special Technical Publication*, 1996,1278:76-88.
- [11] Ganesh Sundara Raman S, Jayaprakash M. Influence of plasma nitriding on plain fatigue and fretting fatigue behavior of AISI304 austenitic stainless steel [J]. *Surf & Coat Techn*, 2007,201(12):5906-5912.
- [12] Caron I, De Monicault J M, Gras R. Influence of surface coatings on titanium alloy resistance to fretting fatigue in cryogenic environment[J]. *Tribology Int*, 2001,34(4):217-236.
- [13] Montross C S, Tao Wei, Lin Ye, et al. Laser shock processing and its effects on microstructure and properties of metal alloys: A review[J]. *Int J of Fatigue*, 2002,24(10):1021-1036.
- [14] Sokol D W, Clauer A H. Applications of laser peening to titanium alloys[C]//ASME/JSME 2004 Pressure Vessels and Piping Division Conference. San Diego, CA: [s. n. ], 2004:36-45.
- [15] Liu K K, Hill M R. The effects of laser shock peening and shot peening on fretting fatigue of Ti-6Al-4V [C]//Fifth International Symposium on Fretting Fatigue. Montreal, Canada: [s. n. ], 2007:105-113.
- [16] Hutson A L, Niinomi A L M, Nicholas T, et al. Effect of various surface conditions on fretting fatigue behavior of Ti-6Al-4V[J]. *Int J of Fatigue*, 2002,24(12):1223-1231.
- [17] Jin O, Mall S, Sanders J H, et al. Durability of Cu-Al coating on Ti-6Al-4V substrate under fretting fatigue [J]. *Surf Coat Techn*, 2006,201(3/4):1704-1712.
- [18] Ruschau J J, Reji J, Thompson S R, et al. Fatigue crack nucleation and growth rate behavior of laser shock peened titanium[J]. *Int J of Fatigue*, 1999,21(S1):199-209.
- [19] Li Qipeng, Li Yonghong, He Weifeng, et al. Application of laser shock processing to improving the fatigue performance of compressor blade[J]. *Advanced Materials Research*, 2010,135:184-189.
- [20] Sano Y, Obata M, Kubo T, et al. Retardation of crack initiation and growth in austenitic stainless steels by laser peening without protective coating [J]. *Mat Sci & Eng*, 2006,417(1/2):334-340.
- [21] Hatamleh O. Laser and shot peening effects on fatigue crack growth in friction stir welded 7075-T7351 aluminum alloy joints[J]. *Int J of Fatigue*, 2007,29(3):421-434.
- [22] Zhang Yongkang, Zhang Shuyi. Investigation of surface qualities of laser shock-processes zones and the effect on the fatigue life of aluminum alloy[J]. *Surf & Coat Techn*, 1997, 92: 104-109.
- [23] Peyre P, Fabbro R. Laser shock processing of aluminium alloys: Application to high cycle fatigue behaviour[J]. *Mat Sci & Eng*, 1996,A210(1/2):102-113.
- [24] Fairand B P, Wilcox B A, Gallagher W J, et al. Laser shock induced microstructural and mechanical property changes in 7075 aluminum[J]. *Appl Phys*, 1972,43(9):3893-3895.
- [25] William F, Bates Jr. Laser shock processing aluminum alloy [C]//Application of Laser in Material Processing. Washington D C: American Society for Metals, 1979:56-60.
- [26] "Aeronautical Manufacture Engineering Handbook" Edits Committee. Aeronautical manufacture engineering handbook[M]. Beijing: Aerospace Industry Press, 1997:119-126. (in Chinese)
- [27] Youneng W, Kysar J W, Yao Y L. Analytical solution of anisotropic plastic deformation induced by micro-scale laser shock peening[J]. *Mechanics of Materials*, 2008,40(3):100-114.
- [28] Rubio-Gonzalez C, Ocan'a J L, Gomez-Rosas G, et al. Effect of laser shock processing on fatigue crack growth and fracture toughness of 6061-T6 aluminum alloy [J]. *Mater Sci & Eng*, 2004, 386(1/2): 291-292.
- [29] Clauer A H, Lahrman D F. Laser shock processing as a surface enhancement process [J]. *Key Eng Mater*, 2001,197:121-142.

# TC6 钛合金激光喷丸纳米组织特性及热稳定性研究

王学德 李应红 李启鹏 何卫锋 聂祥樊 李玉琴

(空军工程大学等离子体动力学实验室, 西安, 710038, 中国)

**摘要:**应用Nd:YAG 高功率激光器对TC6 钛合金试样进行了激光喷丸,对部分强化试样623 K 真空保温10 h。应用原子力显微镜(AFM)、扫描电镜(SEM)、电子背散射电镜(EBSD)、X 射线衍射(XRD)、透射电镜(TEM)等设备对试样强化层形貌和纳米组织进行检测,采用显微硬度计进行显微硬度测量。测试结果表明:TC6 钛合金激光喷丸表面完整性好,未在表面引入微裂纹,表面粗糙度较传统表面强化低;激光喷丸后距离表面 200  $\mu\text{m}$  范围内 $\alpha$ 相在冲击波作用下压缩伸长, $\alpha$ 相和 $\beta$ 相细化,保温后SEM 测试显示强化层组织和强化层深度未发现明显变化;强化后衍射峰变宽,说明强化层发生剧烈塑性变形导致晶粒细化,并留有残余应变,未发现新的衍射峰说明强化过程中没有发生相变;强

化后TC6 钛合金表层产生纳米晶,保温后强化层位错密度降低,纳米晶晶界更加清晰,未发现纳米晶长大;激光喷丸硬度影响层达500  $\mu\text{m}$ ,表面硬度提高12.2%,保温后表面显微硬度降低10 HV<sub>0.5</sub>,硬化深度未发现变化。以上研究表明,TC6 激光喷丸纳米组织和显微硬度在623 K 温度下具有较好的热稳定性,有利于提高钛合金的抗疲劳、抗磨损和抗应力腐蚀的性能,从而突破了美国规范AMS2546 中关于钛合金只能在589 K 温度下应用的限制。

**关键词:**激光喷丸;TC6 钛合金;纳米组织;显微硬度;热稳定性

**中图分类号:**V216.3

(Executive editor: Zhang Huangqun)